CCFE-PR(15)101

C J Ham, I T Chapman, J Simpson and Y Suzuki

Tokamak equilibrium and edge stability when non-axisymmetric fields are applied

Tokamak equilibrium and edge stability when non-axisymmetric fields are applied

C J Ham[1,] I T Chapman[1,] J Simpson[1] and Y Suzuki[2]

[1] CCFE, Culham Science Centre, Abingdon, Oxon, OX14 3DB, UK.
[2] National Institute for Fusion Science, Japan

Tokamak equilibria and edge stability when non-axisymmetric fields are applied

C J Ham[1], I T Chapman[1], J Simpson[1] and Y Suzuki[2]

[1] CCFE, Culham Science Centre, Abingdon, Oxon, OX14 3DB, UK.

[2] National Institute for Fusion Science, Japan

E-mail: christopher.ham@ccfe.ac.uk

Abstract. Tokamaks are traditionally viewed as axisymmetric devices. However this is not always true, for example in the presence of saturated instabilities, error fields, or resonant magnetic perturbations (RMPs) applied for ELM control. We use the VMEC code [Hirshman and Whitson (1983) *Phys. Fluids* **26** 3553] to calculate three dimensional equilibria by energy minimization for tokamak plasmas. MAST free boundary equilibria have been calculated with profiles for plasma pressure and current derived from two dimensional reconstruction. It is well known that ELMs will need to be controlled in ITER to prevent damage that may limit the lifetime of the machine [Loarte *et al Plasma Phys. Control. Fusion* (2003) **45** 1549]. ELM control has been demonstrated on several tokamaks including MAST [Kirk *et al* (2013) *Nucl. Fusion* **53** 043007]. However the application of RMPs causes the plasma to gain a displacement or corrugation [Liu *et al* (2011) *Nucl. Fusion* **51** 083002] . Previous work has shown that the phase and size of these corrugations is in agreement with experiment [Chapman *et al* (2012) *Plasma Phys. Control. Fusion* **54** 105013]. The interaction of these corrugations with the plasma control system (PCS) may cause high heat loads at certain toroidal locations if care is not taken [Chapman *et al* (2014) *Plasma Phys. Control. Fusion* **56** 075004]. VMEC assumes nested flux surfaces but this assumption has been relaxed in other stellarator codes. These codes allow equilibria where magnetic islands and stochastic regions can form. We show some initial results using the HINT2 code[Y Suzuki *et al* (2006) *Nucl. Fusion* **46** L19]. The Mercier stability of VMEC equilibria with RMPs applied is calculated. The geodesic curvature contribution can be strongly influenced by helical Pfirsch-Schlüter currents driven by the applied RMPs. ELM mitigation is not fully understood but one of the factors that influences peeling-ballooning stability, which is linked to ELMs, is a three dimensional corrugation of the plasma edge [Chapman *et al* (2013) *Phys. Plasmas* **20** 056101]. The infinite n ideal ballooning stability of the equilibria with and without the RMPs applied has been calculated using the COBRA code [R Sanchez *et al* (2000) *J. Comput. Phys.* **161** 576-588]. When RMPs are applied, the most unstable ballooning mode growth rate is increased.

Submitted to: *Phys Plasma Control. Fusion*

1. Introduction

Tokamaks have long been thought of as axisymmetric devices and have been modelled as such. Axisymmetry is a key simplifying assumption in the derivation of many of the well known tokamak models. The most basic of these is that magnetohydrodynamic (MHD) force balance in axisymmetry produces the Grad-Shafranov equation for static equilibrium. However, there are many circumstances where tokamaks cannot be assumed to be axisymmetric. These are either due to instabilities produced by the plasma itself, such as tearing modes or the helical core instability, or by applying non-axisymmetric fields to the plasma. We will focus on non-axisymmetric plasmas as a result of applied non-axisymmetric fields. These applied non-axisymmetric fields can be produced either by errors in the alignment of the coils, the so-called error field, or intentionally when resonant magnetic perturbations (RMPs) are applied to control edge-localized modes (ELMs). We will focus here on RMPs for ELM control.

ELMs are periodic eruptions from the plasma edge associated with high confinement mode (H-mode). Whilst ELMs present no danger to current machines it is predicted that natural ELMs would shorten the lifetime of components in ITER [1]. ELMs are finite toroidal, n, and poloidal, m, mode instabilities and are thought to be driven by the peeling-ballooning mode [2]. Axisymmetric stability analysis has shown that H-mode plasmas without RMPs applied sit on the peeling-ballooning stability boundary [3]. The ELM is comprised of filament structures that explode out from the plasma.

ELMs can be controlled using vertical kicks and fueling pellets but we focus on RMPs here. The application of RMPs to an ELMing plasma can have different effects depending on the plasma. In some cases the ELMs are removed completely (ELM suppression), in other cases the frequency of the ELMs can be increased (ELM mitigation). We do not yet have a complete predictive understanding of how ELMs are influenced by RMPs. In this paper we investigate the 'MHD response' on the plasma equilibrium by applying RMPs. This is just the change in magnetic geometry caused by the RMP coils. The pressure and current profiles are not changed by the RMPs. These profiles may well be changed if we took the 'transport response' into account. We then investigate consequent effects on stability of the new non-axisymmetric equilibrium.

The equilibrium resulting from the application of RMPs to an axisymmetric tokamak plasma will be investigated in Section 2. We will use the VMEC code first, which asumes nested flux surfaces. The assumption of nested flux surfaces may be too strong and so we also use HINT2, which allows islands and stochastic regions, to calculate a MAST equilibrium. We also briefly discuss how radial feedback control and equilibrium reconstruction may have to change when we have non-axisymmetric plasmas. In Section 3 we discuss the effect of non-axisymmetry on the edge stability of tokamak plasmas. We calculate Mercier stability and infinite n ballooning stability and we conjecture from this the effect on kinetic ballooning modes (KBMs) and peeling-ballooning modes. The discussion and conclusions are given in Section 4.

2. Equilibrium

There is strong experimental evidence that tokamak plasmas gain a non-axisymmetric character when RMPs are applied. This can be seen at the midplane where non-axisymmetric corruguations appear [4] and at the X-point where a non-axisymmetric lobe structure appears when RMPs are applied [5]. If the plasma is non-axisymmetric and non-helically symmetric there is no Grad-Shafranov equation and equilibrium must be found using other methods. The work by Turnbull *et al* [6] summarizes various methods for calculating the effect on the plasma equilibrium of applying RMP coils. The methods can be categorized as either dynamically evolving the plasma with the coils applied to find the new equilibrium state or by turning the coils on and directly calculating equilibrium states. This method may not find a new equilibrium that is energetically accessible from the initial state though, however it can be significantly faster to calculate. The methods can also be categorized as linear perturbation methods or full nonlinear methods. The RMP perturbation is small so perturbation methods may be sufficient, however nonlinear effects can be significant especially at rational surfaces.

2.1. VMEC

The VMEC code [7, 8] is a fully nonlinear MHD equilibrium code and it has been used extensively throughout the stellarator, reversed field pinch and tokamak communities for calculating equilibrium. The inputs required are the pressure profile and either the safety factor or the toroidal current density as functions of the normalized toroidal flux. Functions are Fourier decomposed in the poloidal and toroidal directions. The code uses a steepest descent algorithm to find the minimum energy states where the plasma energy is given by

$$W = \int \left(\frac{B^2}{2\mu_0} + \frac{p}{\gamma - 1} \right) \mathrm{d}^3 x, \tag{1}$$

where p is the plasma pressure, B is the magnetic field, and γ is the adiabatic index. VMEC does not allow solutions that contain magnetic islands or ergodic regions, only nested flux surfaces.

The code can be run with a fixed or free boundary. The magnetic coil geometry for free boundary runs are input along with the currents in these coils. The full vacuum magnetic field is thus specified for the equilibrium.

2.1.1. MAST equilibria We focus here on a lower single null diverted (LSND) MAST-like equilibrium. We used profiles for plasma pressure and current density based on axisymmetric equilibrium reconstruction. We do not calculate any transport effects from applying the RMP coils so the same profiles are used when RMP coils are switched on. Figure 1 shows the safety factor profile and figure 2 shows the pressure profile used here. The flux surfaces for the VMEC run without RMPs switched on is shown in figure 3.

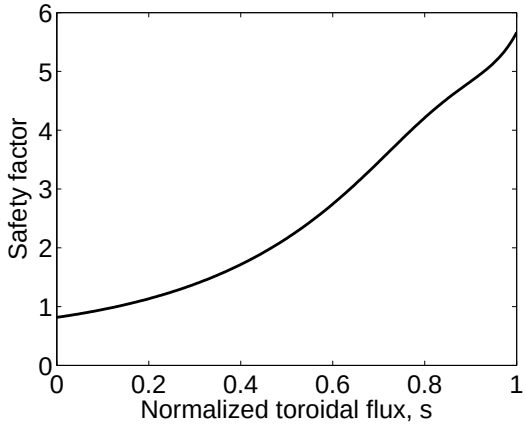

Figure 1. Safety factor profile used in VMEC for the cases with and without RMP coils switch on.

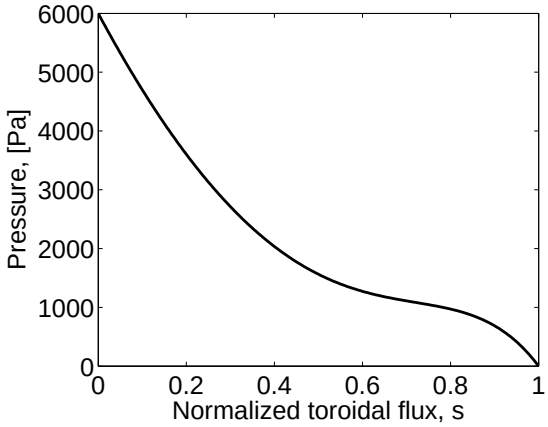

Figure 2. Pressure profile used in VMEC for the cases with and without RMP coils switched on.

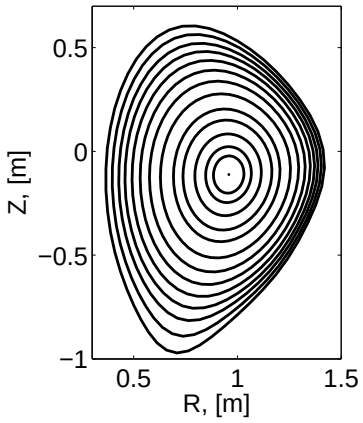

Figure 3. Flux surfaces of the equilibrium calculated by VMEC without RMP coils switched on.

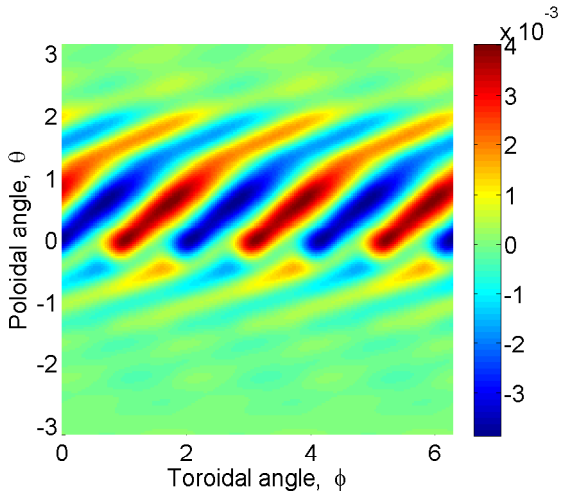

Figure 4. Change in outer flux surface position calculated by VMEC when RMP coils are switched on.

2.1.2. 3D Equilibrium The RMP coils in MAST are positioned in two rows, one above the midplane and one below. There are 12 coils in the lower row and six coils in the upper row, for details of the configuration see [9]. The lower RMP coils are switched on in $n = 2, 3, 4$ and 6 configurations, for LSND plasmas the upper row has little effect and so are not used here. The outer surface of the equilibria with the RMPs applied and calculated by VMEC gains a helical perturbation with toroidal number matching the applied field. Figure 4 shows the displacement caused on the outer flux surface when an $n = 3$ RMP is applied. The $n = 3$ helical perturbations can clearly be seen. The displacement caused by the RMP coils is typically around 1 cm. Other modelling methods, for example MARS-F [10], also predict a helical perturbation to the outer surface of the plasma.

We can also estimate the harmonic content of the displacements caused by the RMP field through the radius of the plasma. The cylindrical R and Z coordinates of the flux surfaces in VMEC are given by

$$R(s,u,v) = \sum_{m,n} R^C_{m,n} \cos(mu + nv) + \sum_{m,n} R^S_{m,n} \sin(mu + nv) \tag{2}$$

$$Z(s,u,v) = \sum_{m,n} Z^S_{m,n} \sin(mu + nv) + \sum_{m,n} Z^C_{m,n} \cos(mu + nv) \tag{3}$$

where s is the normalized toroidal flux and u and v are the normalized poloidal and toroidal angles. We estimate the displacement as

$$\begin{aligned} \xi_{m,n} \sim |R^{C,(RMP)}_{m,n} - R^{C,(NoRMP)}_{m,n}| + |R^{S,(RMP)}_{m,n} - R^{S,(NoRMP)}_{m,n}| \\ + |Z^{C,(RMP)}_{m,n} - Z^{C,(NoRMP)}_{m,n}| \qquad + |Z^{S,(RMP)}_{m,n} - Z^{S,(NoRMP)}_{m,n}|. \end{aligned} \tag{4}$$

Figure 5 shows the estimated harmonics for an $n = 3$ RMP. The low order harmonics penetrate furthest into the plasma. It is expected that the harmonic will decay from the plasma boundary to the core like r^m [11].

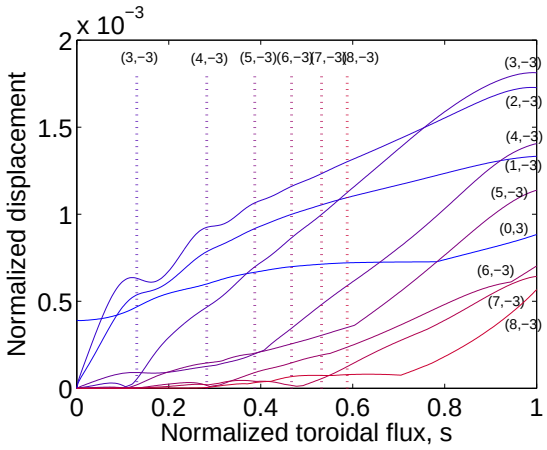

Figure 5. Estimated harmonics of displacements caused by an $n = 3$ RMP field.

2.1.3. Helical Pfirsch-Schlüter currents VMEC assumes nested flux surfaces and an important consequence of this assumption is that helical Pfirsch-Schlüter currents parallel to the magnetic field can arise at rational surfaces where a pressure gradient is present [12–14]. We decompose the plasma current into components parallel , $J_{||}\mathbf{b}$, and perpendicular, $\mathbf{J}_\perp$, to the magnetic field. The force balance equation $\mathbf{J} \times \mathbf{B} = \nabla p$ then implies

$$\mathbf{J}_\perp = \frac{\mathbf{B} \times \nabla p}{B^2}, \tag{5}$$

but we must also satisfy $\nabla \cdot \mathbf{J} = 0$. This requires a parallel current in non-axisymmetry (the helical Pfsirch-Schlüter current) since

$$\nabla \cdot \mathbf{J}_\perp = (\mathbf{B} \times \nabla p) \cdot \nabla \left(\frac{1}{B^2} \right) = -\nabla \cdot \mathbf{J}_{||}, \tag{6}$$

in general does not vanish. If we solve for the parallel current by Fourier expanding $1/B^2$

$$\frac{1}{B^2} = \sum_{m,n} h_{mn}(s) \exp(i(m\theta - n\phi)), \tag{7}$$

we find a divergent Pfirsch-Schlüter current

$$J_{||} \sim \frac{h_{mn}}{s - s_{mn}} \frac{\mathrm{d}p}{\mathrm{d}s}, \tag{8}$$

where s_{mn} denotes the location of the m, n rational surface in normalized toroidal flux. The singularity will be resolved physically by a mechanism beyond the scope of ideal MHD. Boozer [12] suggests that pressure may be flattened at the rational surface by particle diffusion, while Bird and Hegna [13] suggest that enhanced turbulent transport will do this. It is also possible that an island may form which would flatten the pressure gradient and so remove the drive for this current [14]. We plot $|J_{||}|$ in figure 6 for the poloidal and toroidal modes used in our VMEC simulation.

There is also a delta function sheet current that can exist at the rational surfaces. This current is required to prevent island formation in the equilibrium [14].

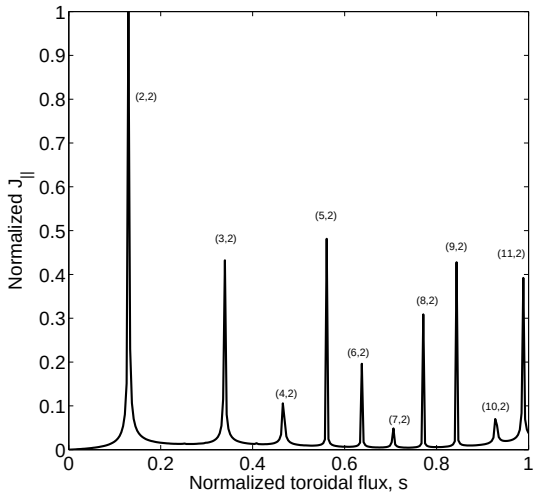

Figure 6. The absolute value of $J_{||}$ calculated for the poloidal and toroidal modes used in the VMEC simulation. The labels indicate the (m, n) pair of poloidal and toroidal mode numbers at the given rational surface.

2.2. HINT2

Islands can form in tokamak equilibria either as a result of applied fields or through instabilities, such as neoclassical tearing modes. VMEC does not allow islands or regions of stochastic magnetic field lines. However, islands and stochastic regions may be very important in determining the plasma response to RMPs. The resulting transport from islands and stochastic regions may also be very important, but that is not considered here. HINT2 [15] is an equilibrium code that can allow islands and stochastic regions to form. It has been used extensively in the stellarator community and more recently for tokamak calculations. HINT2 uses a relaxation method in order to calculate an equilibrium in non-axisymmetry with islands and stochatic regions.

HINT2 has been setup to be run from the outputs of a VMEC equilibrium. We use a case here similar to the LSND equilibrium that we used above. HINT2 uses a two step process to find an equilibrium. The first step relaxes the pressure with a fixed magnetic field so that

$$\mathbf{B} \cdot \nabla p = 0. \tag{9}$$

The second step relaxes the magnetic field so that the following equations reach equilibrium

$$\frac{\partial \mathbf{v}}{\partial t} = -\nabla p + \mathbf{J} \times \mathbf{B} \tag{10}$$

$$\frac{\partial \mathbf{B}}{\partial t} = \nabla \times (\mathbf{v} \times \mathbf{B} - \eta \mathbf{J}) \tag{11}$$

$$\mathbf{J} = \nabla \times \mathbf{B}. \tag{12}$$

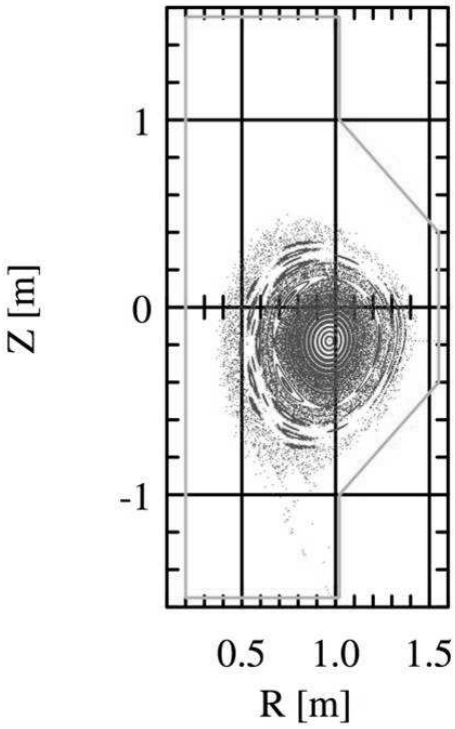

Figure 7. Poincaré plot for a HINT2 equilibrium.

These two steps are repeated until the equilibrium is sufficiently converged. In order to ensure such an equilibrium is well converged, various convergence checks are instigated. The most important check being that the residual force, defined as

$$\text{Residual force} = \frac{|\ \nabla p - \mathbf{J} \times \mathbf{B}\ |}{|\ \nabla p + \mathbf{J} \times \mathbf{B}\ |}, \tag{13}$$

is minimized. We look for this value to drop to or below 1%. Another important check is that the toroidal current stays at a reasonably constant value, close to the experimentally measured toroidal current.

Figure 7 shows the Poincaré plot (plotted using a field line tracing code) for the equilibrium. We can see that islands have formed in the plasma core region consistent with the RMP field applied. We can also see that a stochatic region has formed at the edge of the plasma.

HINT2 does not include plasma rotation effects which may be important [16]. It also does not include two-fluid effects which may determine if islands or stochastic regions are formed [17]. Two-fluid effects have been shown to be important in modelling the influence of RMPs on ELMs using the nonlinear resistive MHD code JOREK [18].

2.3. Other Non-axisymmetric issues

We have not taken into account any transport effects from the application of RMPs. Equilibrium reconstruction of the experiment with RMPs applied would allow us

to validate our theories more accurately. However a non-axisymmetric equilibrium reconstruction code is required for this purpose such as V3FIT [19]. If we try to use axisymmetric methods when we have non-axisymmetric fields then we may have poorly converged equilibria as the toroidal variation in the location of diagnostics will not be included.

The RMPs can also cause rotational braking of the plasma by both $\mathbf{j}\times\mathbf{B}$ torque and neoclassical toroidal viscous torque (NTV) and this has been modelled using MARS-Q [5]. The change in plasma rotation can also change the stability of the peeling-ballooning modes.

The radial feedback control system for ITER will also have to be carefully designed to take non-axisymmetric effects into account. It was shown by Chapman *et al* [20] that the plasma may be moved too close to the metal wall in certain toroidal locations if the radial plasma control does not take into account toroidal variation.

3. Stability

There are a number of approaches to calculating the stability of a plasma with RMPs applied. The nonlinear resistive MHD code JOREK including two-fluid diamagnetic effects, has been used to investigate ELM mitigation on JET with RMPs applied [21]. In these simulations a large ELM was replaced by smaller amplitude ELMs when the RMPs were applied. This was due to the nonlinear coupling between the modes produced by the RMP. Hegna [22] has assumed an equilibrium with RMPs applied is only weakly non-axisymmetric and has used this assumption to calculate the effect of the coupling of toroidal modes on stability. If a representative spectrum of growth rates is assumed then modes were shown to become more unstable.

We now consider the local stability of these plasmas. We investigate local stability because it gives insight into the finite n stability that drives ELMs and it also may give clues to how local modes might change transport in the plasma.

3.1. Mercier stability

Generally tokamaks are stable to interchange modes or Mercier modes. However, the Pfirsch-Schlüter currents can modify the Mercier stability around low order rational surfaces. The Mercier criterion is a necessary condition for linear MHD stability and a sufficient condition for modes localized around a rational surface. The criterion is calculated by VMEC for each flux surface and so this is a very efficient way of investigating stability.

The Mercier criterion in axisymmetry for the large aspect ratio circular cross-section tokamak can be written as [23]

$$\frac{rB_\phi^2}{8\mu_0}\left(\frac{q'}{q}\right)^2 + p'(1-q^2) > 0. \tag{14}$$

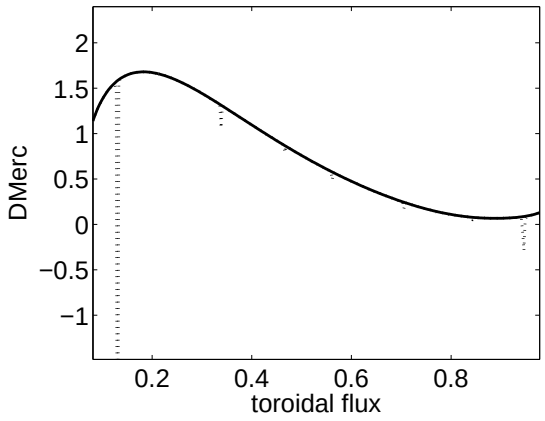

Figure 8. D_M for the case without RMPs (solid line) and with $n = 2$ RMPs applied (dashed line). The equilibrium has become Mercier unstable at these rational surfaces.

The first term is associated with the magnetic shear and is always positive for tokamaks. The $-p'q^2$ is stabilizing and represents the effect of average curvature. This criterion is usually satisfied in a tokamak outside the $q = 1$ surface.

The Mercier criterion has also been calculated in full non-axisymmetric geometry, see for example [24]. It can be decomposed into contributions from different physical effects [24]

$$D_M = D_S + D_I + D_W + D_G > 0 \tag{15}$$

where

$$D_S = \frac{(\Psi''\Phi')^2}{4} \tag{16}$$

$$D_W = \left\langle \frac{gB^2}{g^{ss}} \right\rangle p'V'' - (p')^2 \left\langle \frac{g}{B^2} \right\rangle \left\langle \frac{B^2 g}{g^{ss}} \right\rangle \tag{17}$$

$$D_I = \left\langle \frac{gB^2}{g^{ss}} \left(\Psi'' I' - \Psi'' \Phi \frac{\mathbf{J}\cdot\mathbf{B}}{B^2} \right) \right\rangle \tag{18}$$

$$D_G = -\left\langle \frac{(\mathbf{J}\cdot\mathbf{B})^2}{B^2} \frac{g}{g^{ss}} \right\rangle \left\langle \frac{gB^2}{g^{ss}} \right\rangle + \left\langle \frac{g\mathbf{J}\cdot\mathbf{B}}{g^{ss}} \right\rangle^2 . \tag{19}$$

In these equations $\mathbf{J}$, $\mathbf{B}$ and p are the equilibrium plasma current density, magnetic field and plasma pressure respectively. The toroidal magnetic flux is given by Φ and the poloidal magnetic flux is given by Ψ. The flux surfaces are labelled by s and g is the Jacobian of the transformation. The metric element that appears in the denominator is $g^{ss} = \nabla s \cdot \nabla s$. A prime denotes differentiation with respect to s. The flux surface average of the Jacobian $V' = \int g d\theta d\zeta$ is the magnetic well. The net toroidal current enclosed by a flux surface is I. The angle brackets denote integration over angular variables so $\langle\cdot\rangle = \int\int d\theta d\zeta (\cdot)$.

Here D_S is the contribution from the magnetic field shear, D_W is the contribution from the magnetic well, D_I is the net current contribution and D_G is the geodesic curvature contribution. The Pfirsch-Schlüter currents primarily influence the geodesic

curvature contribution to the Mercier criterion. In fact as can be seen in figure 8 at the rational surface the plasma becomes Mercier unstable. We have not taken into account any effects that will reduce the Pfirsch-Schlüter current here.

The consequences of violating the Mercier criterion has not been calculated here. It is possible that an interchange mode is triggered which may have been seen in experimental observations on sawteeth [25]. It may also be possible that turbulent transport is increased so that the Mercier mode is held at marginal stability as observed in spheromaks by Woodruff *et al.* [26]. Given that the Mercier criterion is violated only at some rational surfaces and that the drive for the instability is the pressure gradient it seems likely for rational surfaces in the core that the Mercier mode would result in enhanced turbulence which would hold the mode at marginal stability. If the Mercier criterion is violated on a rational surface at the edge of the plasma this may destabilize peeling-balooning modes or again enhance turbulent transport and so contribute to 'density pumpout'.

3.2. COBRA

ELMs are thought to be related to peeling-balloning modes which are finite n instabilities. However, we can gain insight into the effect of RMPs on finite n instabilities by looking at infinite n ballooning stability. The formalism for ballooning modes in non-axisymmetric systems has been developed by Dewar and Glasser [27]. We can test the infinite n ballooning stability of our equilibria using the COBRA code [28, 29]. This code uses VMEC equilibria as its input.

We have calculated the infinite n ballooning stability of the case without RMPs applied. The results were axisymmetric. We then apply RMPs and the ballooning mode growth rate gains a toroidal variation of the same toroidal mode number as the applied field. The most unstable mode becomes more unstable. This would indicate that there are certain toroidal locations where the ballooning modes are more unstable. Figure 9 shows a contour plot in radial and toroidal angle space of the ballooning mode growth rate in the edge region with $n = 3$ RMP applied.

Bird and Hegna [13] carried out a study of the effect of small RMP fields on infinite n ballooning modes in tokamak plasmas. They used local non-axisymmetric equilibrium theory and they found that the ideal infinite n ballooning mode stability boundaries were strongly perturbed. Often the most unstable mode was made more unstable, in agreement with our results here.

4. Discussion and Conclusions

4.1. Equilibrium

RMPs for ELM control are an important topic for ITER and future machines. The ELMs need to be controlled so that they do not cause significant material damage but we must make sure that the edge pedestal is not too badly degraded as this could significantly

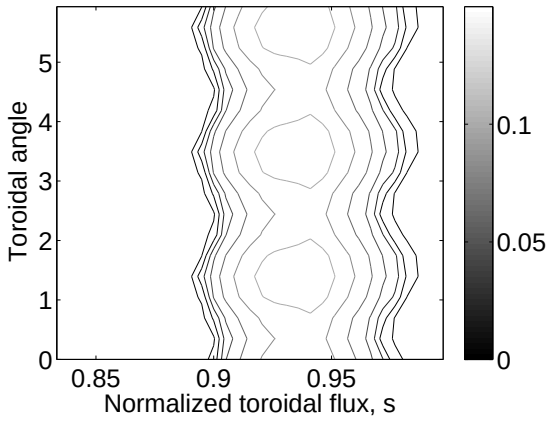

Figure 9. Contour plot of the ballooning mode growth rate against radial and toroidal location.

reduce the fusion power. Experimental results and modelling calculations both indicate that the plasma equilibrium with RMPs applied will gain a non-axisymmetric character. VMEC assumes nested flux surfaces so that islands and stochastic regions cannot form. However this assumption requires singular currents to form at the rational surfaces. It might be expected that physical mechanisms in realistic systems would act to remove these currents for example by pressure flattening at the rational surface. VMEC has some success at calculating similar midplane displacements to those seen in experiments.

HINT2 [15] can calculate equilibria which contain islands and stochastic regions. The initial HINT2 calculation shown in this paper shows a stochastic region at the plasma edge and islands within the plasma. However the version of HINT2 used here does not include plasma toroidal rotation which we would expect to reduce the amplitude of the islands formed or perhaps even suppress them entirely. A version of HINT2 with plasma rotation has recently been used for the first time and we hope to apply it to these problems in the future [30]. The question of what islands appear and at what amplitude is still open and its solution may well require a detailed study of the physics at the rational surface.

The work here only includes the 'MHD response' to the coils being applied. The profiles of pressure and safety factor as a function of toroidal flux are unchanged when the RMPs are switched on. There will also be a 'transport response' which happens over a longer timescale which would alter pressure and safety factor profiles. The 'density pumpout' often seen when RMPs are applied is an example of this.

Non-axisymmetric physics will be important in ITER and it is important that appropriate control systems and experimental reconstruction algorithms are in place. Non-axisymmetric equilibrium reconstruction codes, such as V3FIT, may well be required for plasmas with RMPs applied. The radial feedback control system will have to deal with plasmas which have toroidal variation when the RMP coils are applied.

4.2. Stability

Non-axisymmetric effects can make the plasma more unstable. The Mercier stability criterion for plasmas with RMPs applied was calculated and it was found that there could be a significant change at rational surfaces due to the singular currents there. It is expected that real physical mechanisms would remove this perhaps by enhancing turbulence and flattening the pressure at the rational surfaces. The Mercier modes may well be held at marginal stability. Infinite n ballooning modes also become more unstable at certain toroidal locations. We would conjecture two effects from this. First that finite n peeling ballooning modes, that are thought to drive ELMs, would become more unstable. Second that KBMs (well approximated by infinite n stability) will also become more unstable which would drive more turbulence at the plasma edge and reduce the pedestal pressure gradient.

There is some experimental evidence that both the 'transport response' and the non-axisymmetric stability effect are important when RMPs are applied to a plasma. It is observed that there is a 'density pumpout' reducing the pressure pedestal. However, if an axisymmetric stability analysis is carried out on the plasma profile after pumpout has taken place the plasma is expected to be stable to ELMs whereas in fact it can still have ELMs [3]. This indicates that, in these cases at least, non-axisymmetric effects have made the plasma more unstable to ELMs.

Acknowledgments

We thank S P Hirshman for the use of VMEC and R Sanchez for the use of COBRA. We also thank Y Q Liu, S C Cowley, A Kirk, T M Bird, W A Cooper, J Harrison, P Helander, S Lazerson, S Saarelma and A J Thornton for useful discussions.

This project has received funding from the European Union's Horizon 2020 research and innovation programme under grant agreement number 633053 and from the RCUK Energy Programme [grant number EP/I501045]. The views and opinions expressed herein do not necessarily reflect those of the European Commission. A part of this work was carried out using the HELIOS supercomputer system at Computational Simulation Centre of International Fusion Energy Research Centre (IFERC-CSC), Aomori, Japan, under the Broader Approach collaboration between Euratom and Japan, implemented by Fusion for Energy and JAEA. To obtain further information on the data and models underlying this paper please contact PublicationsManager@ccfe.ac.uk.

References

[1] A Loarte *et al.* 2003 *Plasma Phys. Control. Fusion*, **45** 1549
[2] J W Connor *et al.* 1998 *Phys. Plasmas*, **5** 2687
[3] S Saarelma *et al.* 2011 *Plasma Phys. Control. Fusion* **53** 085009
[4] I T Chapman *et al.* 2014 *Nucl. Fusion*, **54** 083006
[5] I T Chapman *et al.* 2013 *Phys. Plasmas*, **20** 056101
[6] A Turnbull *et al.* 2013 *Phys. Plasmas*, **20** 056114

[7] S P Hirshman and J C Whitson 1983 *Phys. Fluids*, **26** 3553
[8] S P Hirshman *et al.* 1986 *Compu. Phys. Commun.*, **43** 143
[9] A Kirk *et al.* 2013 *Nucl. Fusion*, **53** 043007
[10] Y Q Liu *et al.* 2011 *Nucl. Fusion*, **51** 083002
[11] C J Ham *et al.* 2012 *Plasma Phys. Control. Fusion*, **54** 025009
[12] A H Boozer 1981 *Phys. Fluids*, **24** 1999
[13] T M Bird and C C Hegna 2013 *Nucl. Fusion*, **53** 013004
[14] P Helander 2014 *Rep. Prog. Phys.*, **77** 087001
[15] Y Suzuki *et al.* 2006 *Nucl. Fusion*, **46** L19
[16] R. Fitzpatrick 1998 *Phys. Plasmas*, **5** 3325
[17] F L Waelbroeck *et al.* 2012 *Nucl. Fusion*, **52** 074004
[18] F Orain *et al.* 2013 *Phys. Plasmas*, **20** 102510
[19] J D Hanson *et al.* 2009 *Nucl. Fusion*, **49** 075031
[20] I T Chapman *et al.* 2014 *Nucl. Fusion*, **54** 075004
[21] M Bécoulet *et al.* 2014 *Phys. Rev. Lett.*, **113** 115001
[22] C C Hegna 2014 *Phys. Plasmas*, **21** 072502
[23] J A Wesson *Tokamaks* 2004 Oxford University Press, Oxford, UK, 3rd edition
[24] N Dominguez, J.-N. Leboeuf, B A Carreras, and V E Lynch. 1989 *Nuclear Fusion*, **29** 2079
[25] E A Lazarus *et al.* 2006 *Plasma Phys. Control. Fusion*, **48** L65
[26] S Woodruff *et al.* 2006 *Phys. Plasmas*, **13** 044506
[27] R L Dewar and A H Glasser 1983 *Phys. Fluids*, **26** 3038
[28] R Sanchez *et al.* 2000 *J. Comput. Phys.*, **161** 576
[29] R Sanchez *et al.* 2001 *Comput. Phys. Commun.*, **135** 82
[30] Y Suzuki and Y Nakamura 2014 *Europhysics conference abstracts, 41st EPS Conference on plasma physics, Berlin*, **38F** P4.075